Aeroacoustic Structures within a Supersonic Cavity

John R. Parrish*, Tushar E. Srivastava† and Dr. Kenneth Granlund‡
Department of Mechanical and Aerospace Engineering
North Carolina State University, Raleigh, NC, 27606

This paper presents the results of experiments regarding flow around rectangular cavities at supersonic speeds. Time-resolved fluctuating shear layer, shock waves, and acoustic waves are observed with a shadowgraph optical method and discrete pressure sensors. Results demonstrate differences in the aeroacoustic feedback process between resonance mode and shear layer fluctuation depending on static door positions. Aeroacoustic structures within cavities will be compared with evidence found in previous research studies.

I. Nomenclature

a_0	=	cavity acoustic velocity
α	=	phase lag correction factor
δ	=	boundary layer thickness
δ_0	=	incoming boundary layer thickness
f	=	frequency
γ	=	ratio of specific heats
κ	=	shear layer convection velocity coefficient
L	=	cavity length (=171mm)
M	=	Mach number
M_∞	=	freestream Mach number
n	=	mode number
r	=	recovery factor
U_∞	=	freestream velocity

II. Introduction

The most common representation of flow over an aircraft bay or wheel well is simplified as a rectangular cavity. Flows in this region are a topic of research because they are highly complex with many types of flow structures interacting through a feedback mechanism. The coupled hydrodynamic–acoustic interaction results in semi-harmonic resonance and strong broadband acoustic pressure levels [1]. Rossiter [2] was one of the first scientists to create a theoretical model from experimental data. Using shadowgraph photographs and acoustic pressure sensors for varying cavity length-to-depth ratios (L/D), Rossiter produced the following semi-empirical equation for the Strouhal number, which was corrected by Heller et al.[3] for acoustic temperature recovery:

$$Str_R = \frac{fL}{U_\infty} = \frac{n-\alpha}{M' + \kappa^{-1}} \qquad M' = \frac{M_\infty}{\sqrt{1 + r\left(\frac{\gamma-1}{2}\right) M_\infty^2}} \tag{1}$$

With a door covering the cavity, it is expected that the cavity will experience classical acoustic ("closed box") resonance at the smaller aperture cases, as reported by Bartel [4] and Unalmis [5].

$$f_{ac} = \frac{na_0}{2L} \tag{2}$$

*Graduate Research Assistant, AIAA Student Member.
†Graduate Research Assistant, AIAA Student Member.
‡Assistant Professor, AIAA Associate Fellow.

At supersonic speeds, the imagery of the dynamic opening is of particular interest for aircraft gear bays due to the shear layer and acoustics in this region[6]. These tests can be implemented soon with our current test setup. Schmit [7] imaged a cavity horizontally with shadowgraph photographs, similar to our initial results shown in **Figure 1**.

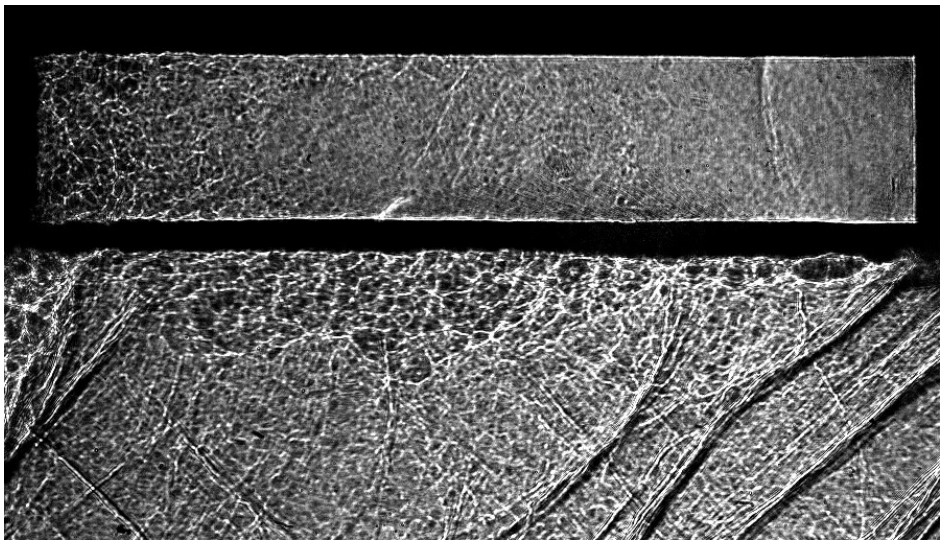

Fig. 1 The image shows initial image quality captured while conducting door fully open tests with an incoming boundary layer δ_0 = .25 inch and Mach 1.5. The image above is a still from a 12,500 fps recording. $\Delta t' = .0500$

III. Setup

A test section was constructed to allow for lateral imaging into the cavity and shear layer visibility. The goal of these tests are to investigate shear layer development with both a static and dynamic opening. The test section was built to offer visibility lateral to the flow allowing shadowgraph imaging. Discrete pressure sensors (Endevco 8507C-15) were installed in the front and aft cavity walls. The optical-access cavity test section has a router blade 50mm in front of the cavity leading edge. The entire cavity test section can be adjusted vertically to split off a portion or all of the tunnel wall boundary layer. A freestream speed of Mach 1.5 and Mach 2.0 will be used when running tests.

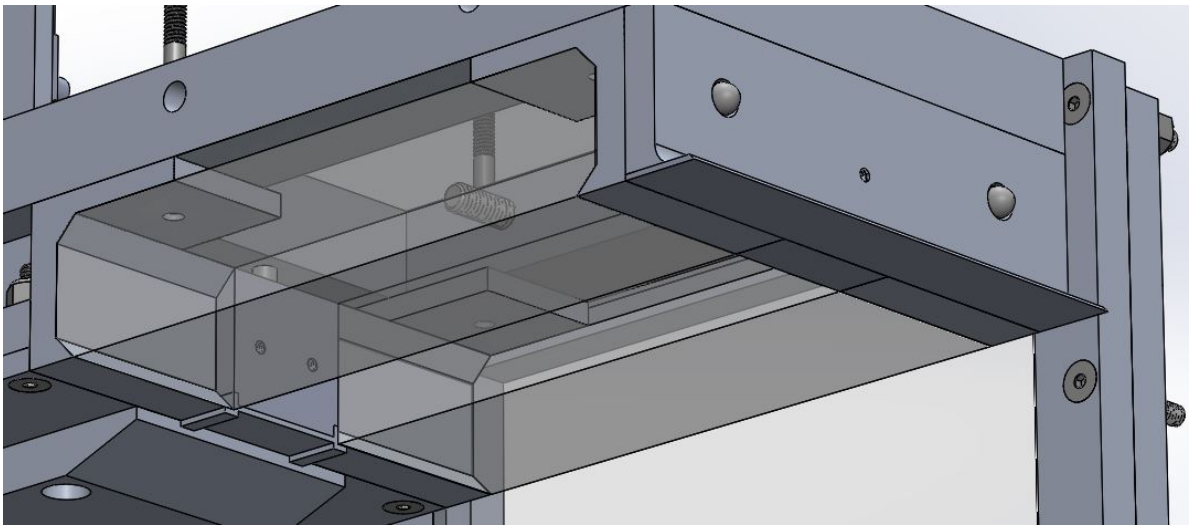

Fig. 2 The newly constructed test section is shown from below in Solidworks.

Figure 3 details the configuration for imaging. For the light source, a laser diode was initially used. The laser was

diverged to illuminate the entire test section. However, it quickly became apparent that coherent light from a laser would not give the desired results. Therefore, an incoherent LED was used in later experiments. Due to the knife edge used to remove the boundary layer, air is bled out of the top of the test section. As a result, a higher stagnation pressure is needed to properly start the tunnel.

The first tests will be conducted with an empty cavity and the door fully open to characterize the resonance at different incoming boundary layers. Discrete pressure data will be correlated to optical imaging of the cavity resonance. The second set of tests will be conducted with the door in different static positions from completely closed to partially covering the cavity to fully open. These results will be compared to the work by Turpin et al.[8]. In the future, imaging will then be done with the addition of a dynamic forward to aft sliding door. Springs will be used due to the lower moving mass weight. Previously, a linear motor was used but this did not produce the desired opening speed.

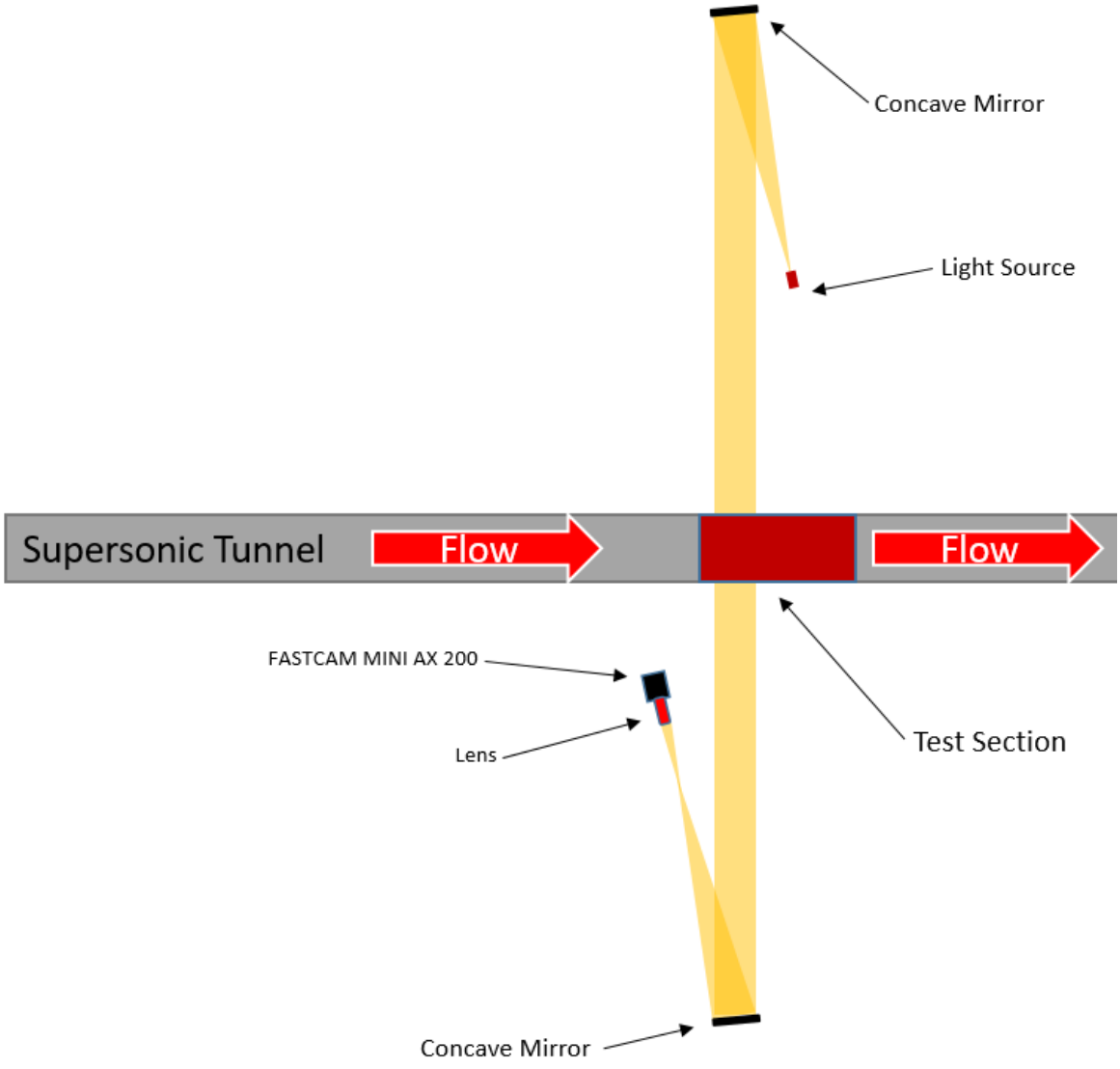

Fig. 3 The diagram shows the setup for shadowgraph imaging.

IV. Results

Initially, the results collected were of sub-optimal quality. In **Figure 1**, the initial results show inconsistent lighting and poor clarity due to using a laser as the light source. Matlab was used to [post] process results by taking the average of several images around what was investigated to remove unwanted disturbances in the visualization.

In **Figure 1**, a number of flow characteristics are worth discussion. Firstly, the tunnel is capable of starting at Mach 1.5 using the test section designed. [The diagonal shocks at the front of the cavity demonstrate the tunnel is properly starting.] Secondly, the shear layer is seen separating at the cavity opening. [Additionally, the knife edge is operating as intended by evidence of the thin boundary layer at the front of the cavity. The cavity and knife edge were placed at a distance of $\delta = .25$ inch from the wind tunnel ceiling. As a result, the boundary layer is very thin as seen in the results allowing for a clearer representation of the separated shear layer. Finally, acoustic resonance is visible along the top of the cavity surface. Acoustic waves are visible in **Figure 1** and **Figure 4** along the top surface of the cavity.

A. Internal Acoustic Structures

A main goal was to investigate previous models describing acoustic resonance of cavities. One such model described previously was Rossiter's model. [This model] assumes shear vortices are shed from the front edge of the cavity and travel downsteam. After traveling downstream, they impact the aft wall and produce pressure waves that travel upstream.

The structures observed in the experiment build on this model and fills in more detail as to what occurs within the cavity. Schmit [7] showed that entrainment structures exist in open cavities and move towards the aft wall before impacting. The results below show this phenomenon when a static door is introduced. The table below describes the movement of acoustic structures in the cavity.

Table 1 Flow features of the cavity at Mach 1.6

Feature	Description
1	An entrained air structure is seen moving from the freestream flow into the cavity.
2	The structure impacts the floor of the cavity and reflects to form a V shape.
3	The faint right structure is a produced acoustic wave. The left structure is a previously produced acoustic wave that has reflected and is traveling upstream.
4	The faint structures are now more pronounced as they move apart.
5	Both structures move into the corners and near the wall. Note the right (aft) structure is not a plane wave.
6	Both structures have now reflected off of the front and aft walls. The aft wall reflection produces a non-planar reflection as a result of its original curved geometry.
7	In yellow, a vortex bubble has formed due to the impact at the front wall. The two waves are seen to continue to move towards the center.
8	The left wave is no longer visible. The wave circled in red is traveling from the aft wall to the front wall which is towards the right in this image. As it interacts with the freestream flow, it is bent by this relative motion of the flow. In addition, this interaction appears to impact the shear layer. The structure circled in yellow is the acoustic wave propagating into the freestream flow.
9	The red structure is the forward traveling acoustic wave. The yellow structure is an entrained air structure beginning to become visible just as was seen in Case 1.
10	The structure impacts the floor of the cavity and repeats the acoustic process all over again.

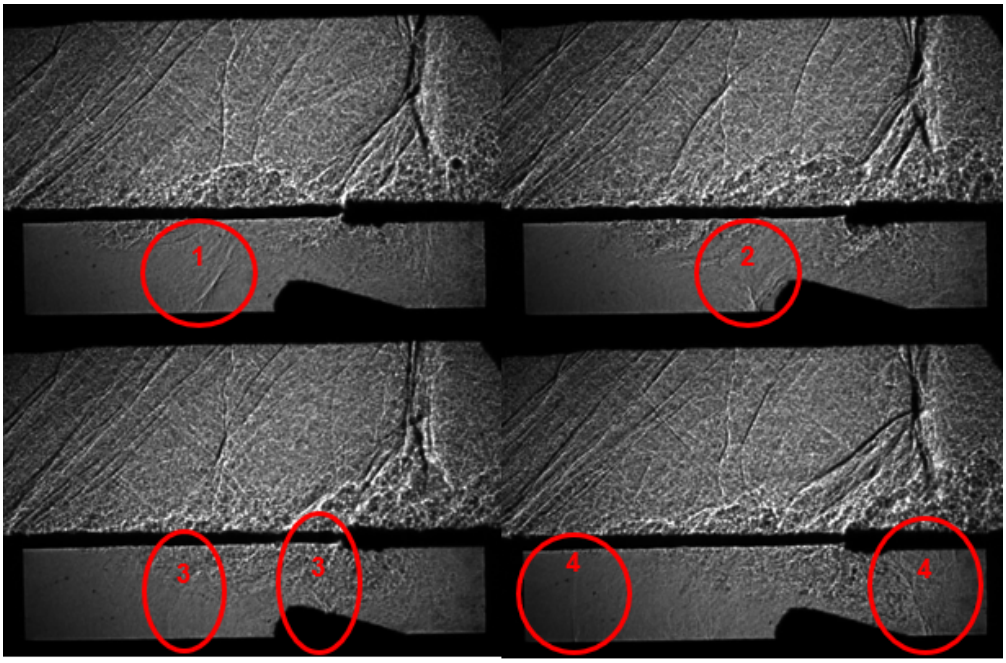

Fig. 4 Collection of images showing the propagation of structures within the cavity recorded at 100kHz and at Mach 1.6

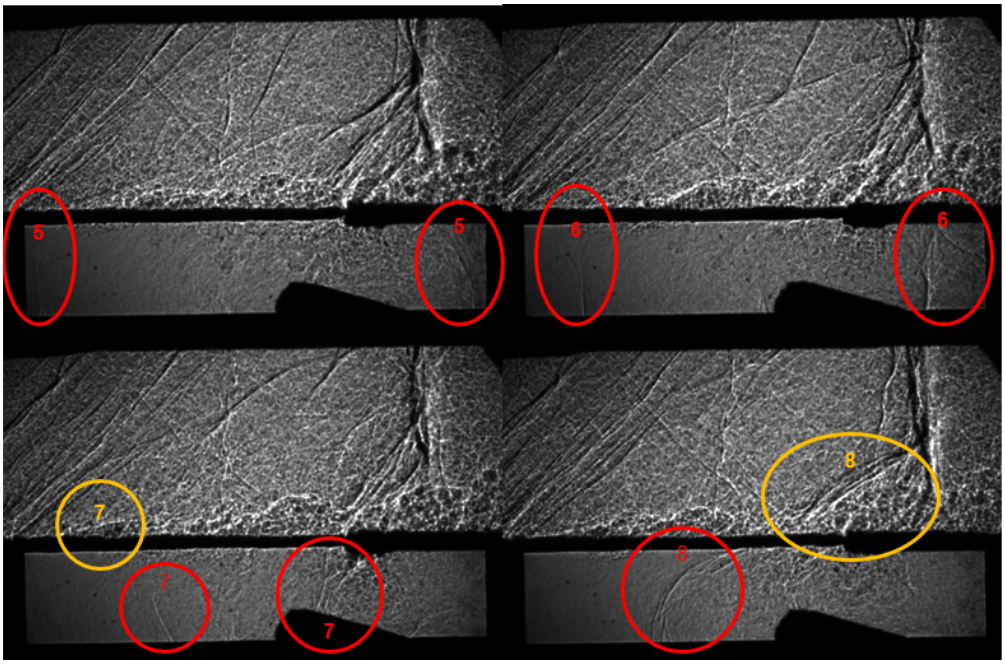

Fig. 5 Collection of images showing the propagation of structures within the cavity recorded at 100kHz and at Mach 1.6

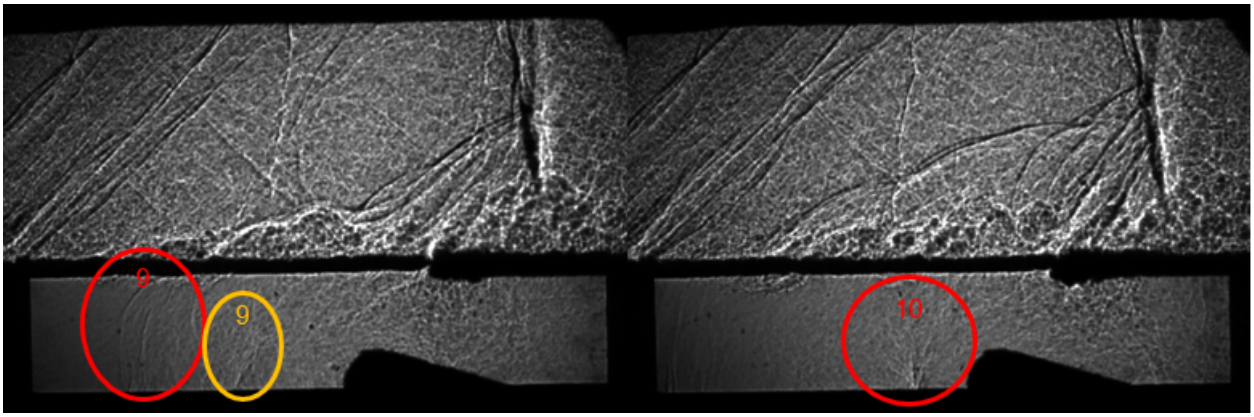

Fig. 6 Collection of images showing the propagation of structures within the cavity recorded at 100kHz and at Mach 1.6

Figures 4 - 6 demonstrate how the acoustic waves produce vortices. The acoustic wave shown as an example in **Figure 4** is stronger than most observed. These results match what Schmit [7] found regarding vortex formation. Improvements in the light source and the addition of a dynamic moving door resulted in **Figure 7** and **Figure 8**. These schlieren results are still not as clear as desired and as result, the authors will continue to use shadowgraph. Also note the disruption in the shear layer in **Figure 8** just after the leading edge due to the acoustic wave impact.

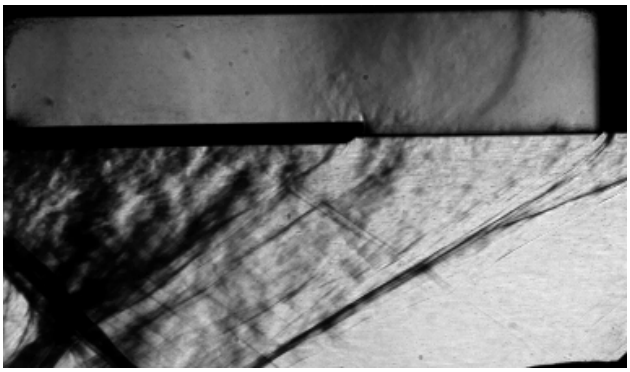

Fig. 7 Freestream flow moves right to left. The schlieren image was taken at 100,000 fps depicting an acoustic wave moving from left to right (upstream) shown in dark. Conditions were δ_0 = .25 inch and Mach 2.

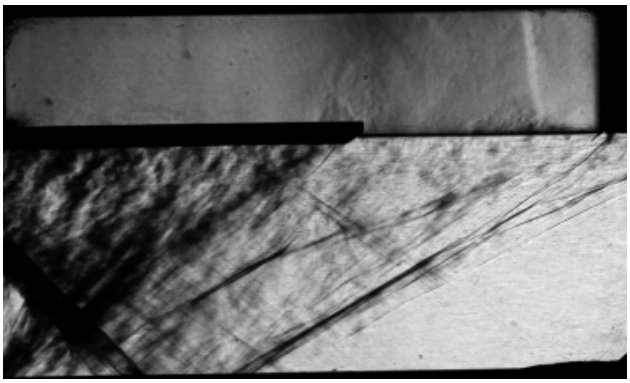

Fig. 8 Freestream flow moves right to left. The schlieren image was taken at 100,000 fps depicting a reflected acoustic wave from the previous figure moving from right to left (downstream) shown in white. An unsteady region is seen just after of the front wall as seen previously. Conditions were δ_0 = .25 inch and Mach 2.

B. Structure Speed

The speed of previously discussed structures are helpful to determine additional properties of the structures. Using the 100kHz image data, an average speed of these structures can be determined over multiple frames. To minimize the effects of the shear layer, the reference point used to measure the position was placed at the floor of the cavity. In this area, it is known that re-circulation effects are active and likely contributing to the difference in acoustic velocity[9]. It is observed that acoustic waves traveling downstream are notably slower as they propagate into re-circulation.

Direction of Travel	**Upstream**	**Downstream**
Mean (m/s)	416.33	339.46
Standard Deviation	46.0647269	38.70366028
Number of Samples	20	20

V. Future Improvements

The addition of a dynamic sliding door introduced new challenges. The small gap between the door and aft wall become a source of drag. Therefore, the linear motor used to open the door was too weak to produce a satisfactory opening time less than 25 milliseconds. Adjusting for drag, the motor would still not be able to reach the desired opening time. As a result, springs will be used to reach the desired opening speed and the gap will be further sealed.

Additional improvements will be needed to the imaging setup to allow for a sharper acoustic wave detection. Pressure transducers had been used during tests, but sharper wave detection and higher sample rate transducer equipment will be needed to relate pressure data to the images recorded.

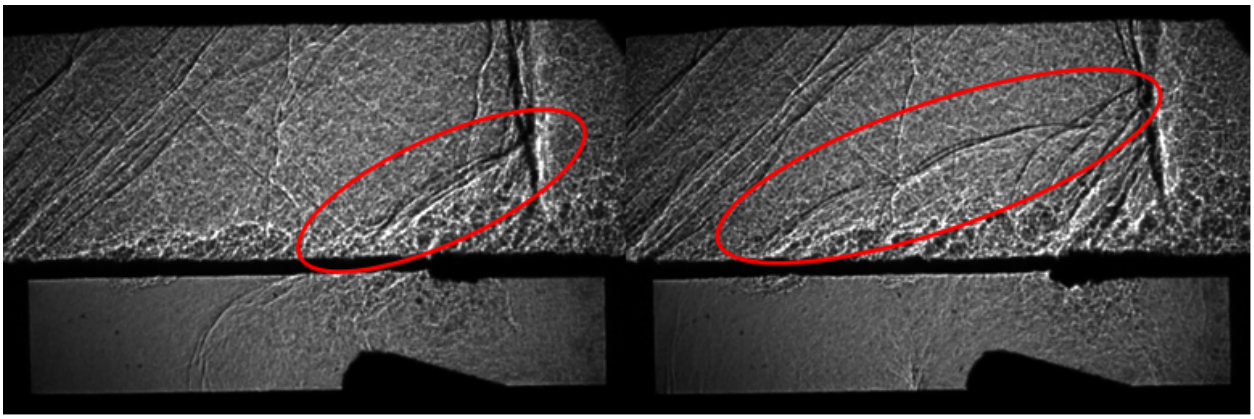

Fig. 9 Collection of images showing the propagation of structures within the cavity recorded at 100kHz and at Mach 1.6 showing the propagation of the acoustic wave into the freestream.

VI. Conclusion

From the data collected so far, a [couple of observations] can be made. The cavity acoustic structures propagate into the freestream and interact with the shear layer. Clearer and more tests are needed to further investigate how these layers interact. Currently, glass bevels obstruct clear vision along the cavity waterline. In addition, damage to the glass due to the door needs to be addressed. It is also confirmed that the tunnel is starting properly and that acoustic resonance is occurring. Higher quality pressure transducers will confirm the results of other cavity flow results observed by Turpin[8]. These sensors will also be useful to track acoustic waves within the cavity. These pressure sensors will also allow for the ability to acquire time resolved data.

Acknowledgements

This work is funded by AFOSR Grant No. FA9550-20-1-0199 DEF with [Gregg Abate] as the Program Officer.

References

[1] Tracy, M. B., and Plentovich, E. B., "Cavity unsteady-pressure measurements at subsonic and transonic speeds," Tech. Rep. NASA TP-3669, 1997.

[2] Rossiter, J. E., "Wind-Tunnel Experiments on the Flow over Rectangular Cavities at Subsonic and Transonic Speeds," *Aeronautical Research Council*, Vol. Rept. 3438, 1966.

[3] Heller, H., Holmes, D., and Covert, E., "Flow-induced pressure oscillations in shallow cavities," *Journal of Sound and Vibration*, Vol. 18(4), 1971.

[4] Bartel, H. W., and McAvoy, J. M., "Cavity Oscillation in Cruise Missile Carrier Aircraft," Tech. Rep. AFWAL-TR-81-3036, 1981.

[5] Unalmis, N. T., O. H.and Clemens, and Dolling, D. S., "Cavity oscillation mechanisms in high-speed flows," *AIAA Journal*, Vol. 42, No. 10, 2004, pp. 2035–2041. https://doi.org/10.2514/1.1000.

[6] Johnson, R. A., Stanek, M. J., and Grove, J. E., "Store separation trajectory deviations due to unsteady weapons bay aerodynamics," *AIAA*, Vol. Paper No. 2008-118, 2008.

[7] Schmit, R. F., Grove, J. E., Semmelmayer, F., and Haverkamp, M., "Nonlinear Feedback Mechanisms Inside a Rectangular Cavity," *AIAA*, Vol. 52(10), 2014.

[8] Turpin, A., Granlund, K., Hayashi, T., and Sakaue, H., "Supersonic Cavity Flow with a Downstream-Sliding Door," *Experiments in Fluids*, Vol. 62, No. 239, 2021.

[9] Schmit, R. F., Grove, J. E., Semmelmayer, F., and Haverkamp, M., "Examining passive flow control devices with high speed shadowgraph images around a Mach 1.5 cavity flow field," *Air Force Research Laboratory*, 2012.